The Role of Overwash in the Evolution of Mixing Zone Morphology Within Barrier Islands

By: William Anderson and Rachel Lauer

Abstract: Overwash is a major controlling factor in the morphology of the mixing zone of coastal aquifers. Conceptual models of the mixing zone describe an interface controlled by tidal oscillations, wave run-up, and other factors; however, few describe the influence of large storm events. In August 1993, Hatteras Island, North Carolina, USA, experienced a 3-m storm surge due to Hurricane Emily. Sound-side flooding infiltrated a wellfield, causing a dramatic increase in TDS levels that persisted for more than 3 years. Two-dimensional simulations with SUTRA, the USGS finite-element model, are calibrated to the TDS breakthrough data of this storm to infer model dispersivity values. Simulations using the calibrated dispersivity values, predicted flooding levels, and 54 years of hurricane records to determine the influence of the overwash events suggest that it is rare for the mixing zone to approximate the conceptual morphology. Even during quiescent periods such as between 1965 and 1975, TDS levels do not return to theoretical levels before being elevated by a subsequent storm event. Thus, while tidal oscillations and other factors are important to mixing zone development, basic wind events and more severe storm events may have more influence and lasting effect on the morphology of the mixing zone.

Anderson, William P., Jr. Lauer, Rachel M. *(2008) HYDROGEOLOGY JOURNAL. The Role of Overwash in the Evolution of Mixing Zone Morphology Within Barrier Islands. DOI: 10.1007/s10040-008-0340-z. ISSN: 1431-2174

The role of overwash in the evolution of mixing zone morphology within barrier islands

William P. Anderson Jr. · Rachel M. Lauer

Abstract Overwash is a major controlling factor in the morphology of the mixing zone of coastal aquifers. Conceptual models of the mixing zone describe an interface controlled by tidal oscillations, wave run-up, and other factors; however, few describe the influence of large storm events. In August 1993, Hatteras Island, North Carolina, USA, experienced a 3-m storm surge due to Hurricane Emily. Sound-side flooding infiltrated a wellfield, causing a dramatic increase in TDS levels that persisted for more than 3years. Two-dimensional simulations with SUTRA, the USGS finite-element model, are calibrated to the TDS breakthrough data of this storm to infer model dispersivity values. Simulations using the calibrated dispersivity values, predicted flooding levels, and 54years of hurricane records to determine the influence of the overwash events suggest that it is rare for the mixing zone to approximate the conceptual morphology. Even during quiescent periods such as between 1965 and 1975, TDS levels do not return to theoretical levels before being elevated by a subsequent storm event. Thus, while tidal oscillations and other factors are important to mixing zone development, basic wind events and more severe storm events may have more influence and lasting effect on the morphology of the mixing zone.

Introduction

Barrier islands provide a unique opportunity for hydrogeologists to evaluate the dynamic interface between saltwater and fresh groundwater. In these systems, a combination of factors leads to the development of a freshwater lens, where freshwater sits on top of the relatively dense saltwater beneath. Many studies have focused on elucidating factors that contribute to the configuration and morphology of the freshwater lens, starting with the independent studies conducted by Ghyben (Drabbe and Badon Ghyben 1888–1889) and Herzberg (1901) at the beginning of the nineteenth century. Their early work was motivated by the need to acquire fresh water for water supply without perturbing the saltwater–freshwater interface, which persists as a common modern groundwater concern for hydrogeologists dealing with water supply in coastal areas. Their contribution was recognized in the form of the Ghyben-Herzberg principle (see, for example, Bear 1972 for a detailed explanation of this relationship), which empirically relates the depth of the interface to the elevation of the land surface under a set of simplifying assumptions.

A primary assumption of the GH-principle is that the system under consideration is static, not dynamic as is the case in any coastal tidally influenced system. Additionally, it is assumed that the interface represents a sharp boundary rather than a gradational change from saltwater to fresh groundwater. In reality, the interface is not a sharp boundary, but a dynamic boundary, or mixing zone where the lateral transition from saltwater to freshwater is influenced by many factors. Some of these factors include: daily tidal fluctuations, seasonal changes in recharge/discharge, the proximity of pumping wells and the volume withdrawn, wave run-up, and overwash events that can occur during tropical storms and hurricanes. While overwash and coastal flooding have been suggested as a significant contributor to aquifer salinization (Anderson 2002), this mechanism of salinization has received scant attention in the literature. The location, lateral extent and configuration of the mixing zone are influenced by local conditions, and recent research suggests that many coastal systems depart entirely from the traditional freshwater lens underlain by a saltwater wedge commonly depicted in textbooks (Freeze and Cherry 1979; Domenico and Schwartz 1990).

Research conducted in the western Belgian coastal plain (Vandenbohede and Lebbe 2006) indicates that a dynamic

equilibrium can develop between the saltwater and freshwater in the form of an inverse density distribution, if the beach geometry is favorable, consists of a gentle slope, or the area experiences large tidal oscillations. Beach geometry can therefore profoundly impact the lens configuration as it may favor wave run-up associated with overwash, contributing to the infiltration of saltwater farther inland, especially during high tides. Another departure from the traditional lens development was noted in the coastal bays of the Delmarva Peninsula (Delaware, Maryland, and Virginia), where geophysical surveys identified freshwater plumes that extend over 1-km from the shoreline, where they ultimately discharge into the estuary rather than forming the traditional "lens" (Krantz et al. 2004; Manheim et al. 2004). In this case, the hydraulic conductivity distribution, or the presence of semi-confining units, is thought to be responsible for the anomalous discharge pattern.

Recent events such as Hurricane Katrina in 2005 and the Asian tsunami in 2004 have provided the impetus for further research into the effects of overwash on water quality as warmer temperatures and the concomitant increase in tropical storms and potential overwash events occur. Previous work conducted on Hatteras Island, North Carolina (Anderson 2002), evaluated the effects of overwash on water quality in the aftermath of Hurricane Emily, which inundated the sound side of the island in 1993. This region is particularly susceptible to severe storms, and the predictive simulations conducted by Anderson (2002) suggest that multiple overwash events could have a persistent impact on water quality, with elevated chloride levels observed for as much as 3 years after Hurricane Emily. The current study is designed to further evaluate the effect of storm events in addition to basic wind events, as it is suspected that these factors may have a more profound role in mixing zone morphology than previously considered.

Hydrogeologic setting

The study area is located on Hatteras Island, a barrier island within the Outer Banks of North Carolina and the Cape Hatteras National Seashore (Fig. 1). This study specifically evaluates the Cape Hatteras region and the Buxton Woods aquifer, where the island shifts from a N–S trend to an E–W trend, and widens to approximately 3 km from the Atlantic Ocean to Pamlico Sound. This region has been the subject of multiple previous investigations (Burkett 1996; Anderson et al. 2000; Anderson 2002) which have successfully constrained the hydraulic parameters of this system, making it an ideal location for the modeling study presented here.

The Buxton Woods aquifer consists of two units with a total thickness of approximately 24 m (Burkett 1996). The upper Buxton Woods aquifer (Heath 1988; Heath 1990) comprises highly permeable medium-to-coarse-grained sand with lenses of shell fragments. The lower Buxton Woods aquifer comprises medium-to-coarse-grained sand with lenses of shell hash and shells, and extends from 15 to 24 m in depth. There is a thin layer between the upper and lower aquifers between 12 and 15 m in depth consisting of less permeable, fine-grained sand and silts. The lower Buxton Woods aquifer is underlain by a 13 m thick unit that ranges from silty to clayey sand, and is considered more competent and less permeable than the semi-confining layer that separates the upper and lower aquifers. This basal unit is treated as a no-flow boundary in the present modeling study. The freshwater lens on the island varies with storm events, but in general it contains a thin mixing zone that is truncated at depth (~24 m) by a confining layer and is just less than the width of the island (Heath 1988; Heath 1990). The hydraulic parameters of the Buxton Woods aquifer were estimated from evaluation of late-time pumping data obtained during a 72-h aquifer test (Burkett 1996). Water levels were monitored throughout the test using two fully penetrating monitoring wells and wells screened at various depths within the upper and lower aquifers. Aquifer parameters derived from the late-time data indicate a bulk aquifer transmissivity of 0.0060 m^2/s and a storativity of 0.15. Mean recharge rates based on water levels at the middle of transect 2 (Anderson and Evans 2007) are estimated to be 2 mm/d (0.079 kg/s). These data also reveal anisotropy within the aquifer, with the horizontal permeability of the aquifer

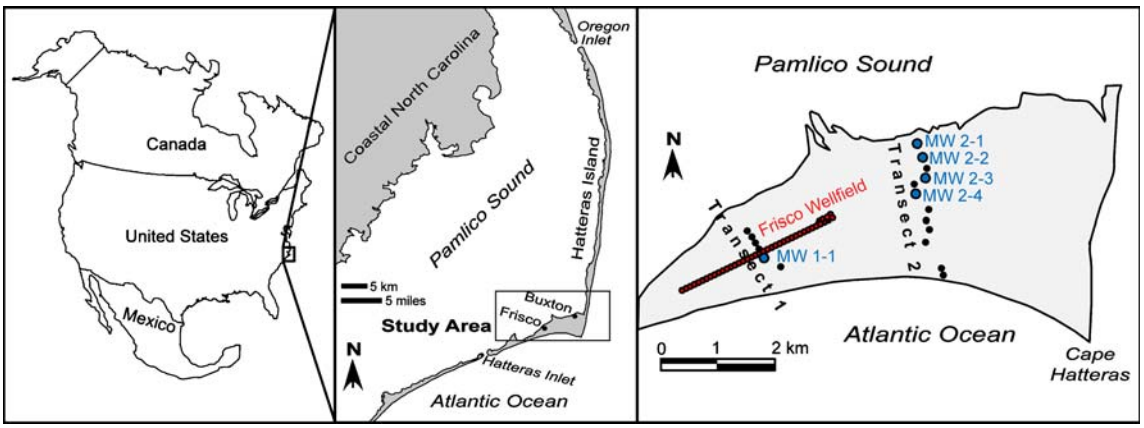

Fig. 1 The location of the Outer Banks barrier-island chain in eastern North Carolina, USA. The study focuses on the southern portion of Hatteras Island

nearly four times the vertical permeability. See Table 1 for calibrated aquifer parameters used in the present study.

Surface drainages constructed in the Cape Hatteras region were designed to discourage mosquito habitat and mitigate seasonal flooding by draining excess surface water into Pamlico Sound or, more rarely, the Atlantic Ocean. Surface drainage is non-existent during the summer months and when dry conditions exist during other seasons. There is an unknown drainage rate during high water-table conditions in the interdunal swale along the north side of the island. It is suspected, however, that, on the sound side of the island, the interdunal swales may also enhance sound-side flooding, as they provide a direct conduit from Pamlico Sound during storm events, when storm surge levels are capable of carrying saline water up to 1 km inland (Anderson 2002). While several of these interdunal swales have been deepened as described above, they are still natural features and can also serve as an overwash conduit on undisturbed islands. The large size of Pamlico Sound (~120×40 km), its isolation from the Atlantic Ocean through barrier-island development, and its alignment with the prevailing winds (NE in the summer and SW in the winter) makes it particularly susceptible to seiching, or oscillations in water levels resulting from the development of a standing wave, even during benign weather conditions (Luettich et al. 2002). The persistence of seiching in this region has been well documented (Roelofs and Bumpus 1953; Pietrafesa et al. 1986; Luettich et al. 2002), although the impact of this phenomenon on mixing zone morphology due to overwash has not been previously considered.

Model setup

This study uses the US Geological Survey finite-element code SUTRA (Voss 1984; Voss and Provost 2002) to simulate two-dimensional groundwater flow and solute transport within the Buxton Woods aquifer. SUTRA was chosen for these simulations because it is one of many codes that is applicable to unconfined coastal aquifers and is capable of simulating variable-density fluids and fluctuating upper boundaries. SUTRA is well tested and has been applied to a variety of coastal settings (see, for example, Voss and Souza 1987; Underwood et al. 1992; Collins and Easley 1999; Li et al. 2000; Wilson and Gardner 2006) including the Buxton Woods aquifer (Anderson 1999; Anderson et al. 2000). Two-dimensional simulations were deemed adequate given the nature of the site. The island is roughly linear in the region of both transects. In addition, transect 1 perpendicularly bisects the Frisco Wellfield, which consists of a line of 42 wells spaced at a regular distance of 76.2 m. Only at the far eastern end of the wellfield is there a second line of wells (Fig. 1).

Table 1 Aquifer parameters used to calibrate groundwater flow and solute transport simulations at transects 1 and 2

Parameter	Value
Maximum permeability (m^2)	2.7×10^{-11}
Minimum permeability (m^2)	6.6×10^{-12}
Porosity	0.20
Longitudinal dispersivity in maximum permeability direction (m)	10
Longitudinal dispersivity in minimum permeability direction (m)	5
Transverse dispersivity in maximum permeability direction (m)	1
Transverse dispersivity in minimum permeability direction (m)	1
Model thickness (m) – transect 1	76.2
Model thickness (m) – transect 2	1.0

Simulations described in this study were performed along two cross-island transects: calibration simulations along transect 1, and historical simulations along transect 2. Transect 1 was chosen for the calibration because wells at the center of the transect remove water that is the source of a total dissolved solids (TDS) breakthrough curve. Historical simulations were not performed along transect 1 because that would necessitate detailed pumping information from the early 1960s to the present and these data do not exist. An advantage of using transect 2 for demonstrations of the effect of overwash on the mixing zone is the lack of pumping in the vicinity. Furthermore, transects 1 and 2 are similar hydrogeologically: they have similar aquifer parameters (Burkett 1996; Heath 1988; Heath 1990) and borehole geophysical logs (Anderson 1999; Heath 1988; Heath 1990). Because the two transects are similar, the choice was made to calibrate dispersivity to the data at transect 1, and then use those dispersivity data in historical simulations along transect 2.

Initial test simulations utilized the island half-width with a no-flow boundary condition at the groundwater divide; however, large variations in sound-side water levels during simulated flooding events reversed hydraulic gradients and caused reflections off of the no-flow boundary at the centerline of the island. Therefore, all simulations described in this paper incorporate full island widths. Both model domains comprise a 24-m-thick aquifer that extends laterally into both the Atlantic Ocean and Pamlico Sound 1,000 m beyond the width of the island, which are 2,400 and 3,400 m at transects 1 and 2, respectively (Fig. 2). Both model domains assume a no-flow boundary at the base of the aquifer (Burkett 1996) and approximate local topography at the top of the model domain. Lateral boundaries at both transects constitute hydrostatic pressure, as does the upper boundary corresponding to the Atlantic Ocean and Pamlico Sound. At the lateral and upper boundaries representing the Atlantic Ocean, hydrostatic pressure remains constant throughout all simulations and incorporates a constant seawater-mass concentration of 0.0357 kg/kg. At the lateral and upper boundaries representing Pamlico Sound, hydrostatic pressure varies with simulated storm events and incorporates a mass concentration of 0.019 kg/kg, which is typical of this region of the sound (Wilder et al. 1978; Giese et al. 1979). The pre-storm elevation of Pamlico Sound lies 0.15 m above MSL. Simulations do not include tidal fluctuations at either lateral boundary given the microtidal (less than 1 m of tidal amplitude)

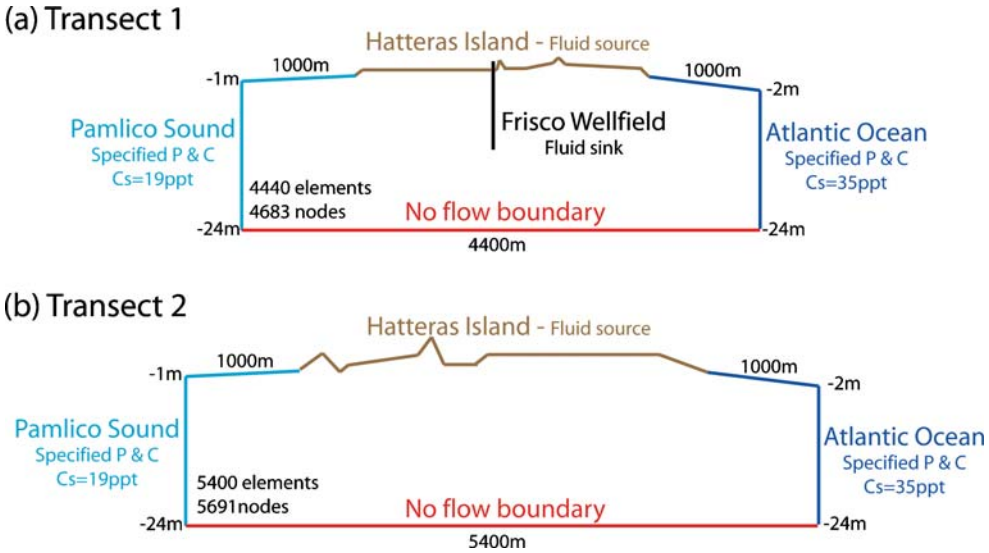

Fig. 2 The model domains used in simulations of **a** transect 1 and **b** transect 2

nature of the Cape Hatteras region, especially within Pamlico Sound (Anderson 1999; Anderson et al. 2000).

The model domain of transect 1 consists of 4,683 nodes and 4,440 elements that bisect the linear Frisco Wellfield, which experienced approximately 2.5 m of sound-side flooding during Hurricane Emily in 1993 (Peng et al. 2004). At the time of the hurricane, the wellfield consisted of 42 pumping wells with a spacing of 76.2 m and was located in an interdunal swale with a land surface elevation approximately 1 m above MSL (mean sea level). The screened depths of all wells in the wellfield, which lie approximately at the midpoint of the island in a linear orientation that parallels the trend of the island, are between 3 and 11 m below MSL when including the gravel pack in the screen length. The model domain of transect 2 consists of 5,691 nodes and 5,400 elements and bisects the island at its widest point, where approximately 3.2 m of sound-side flooding occurred (Peng et al. 2004). Simulations were run along this transect because of a wealth of water-table elevation and aquifer parameter data, including transmissivity and storativity values (Burkett 1996). Additionally, there are no pumping wells along this transect; thus, there are no ambiguities regarding pumping schedules over the course of the historical simulations.

For both transects, initial conditions reflect pre-storm conditions generated with a 1,500-year cold-start simulation in which the entire aquifer has an initial seawater mass concentration. Initial time steps of one second expanded gradually at a rate of 1.01 to a maximum time step of one week at late times during the simulation, giving a total of approximately 79,000 time steps during the 1,500 years of simulation. Recharge rates for both transects were calibrated during the initial conditions simulations to known pre-hurricane water levels. Simulations at transect 1 included one pumping well removing water at an average rate of 0.757 L/s (J. Coleman, Cape Hatteras Water, personal communication, 1996).

Model calibration simulations

Simulations at both transects were calibrated to known field observations utilizing the aquifer parameters shown in Table 1. In simulations along transect 1, longitudinal and transverse dispersivities were calibrated to TDS breakthrough data that were attributed to sound-side flooding during Hurricane Emily (J. Coleman, Cape Hatteras Water, personal communication, 1996). These data reflect TDS concentrations in the raw water entering the water treatment plant (Fig. 3). The raw water represents the mean TDS concentration of the 42 pumping wells that were in use during the days following the hurricane. Given the similar hydrogeologic position of the pumping wells in terms of surface elevation and screen depth, as well as the location of the simulation at the midpoint of the linear wellfield as an average condition in the aquifer, this is an adequate characterization for the demonstrative goals of this paper. Calibrated dispersivities from transect 1 were used at transect 2, where breakthrough data do not exist. Calibration at transect 2 involved matching observed and simulated water levels prior to and in the months following the hurricane.

Pamlico Sound water levels varied considerably during Hurricane Emily (Peng et al. 2004). Figure 4 shows the

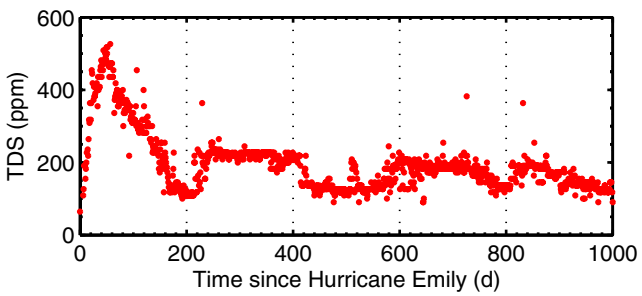

Fig. 3 The TDS breakthrough data as measured at the Frisco Wellfield after Hurricane Emily in 1993

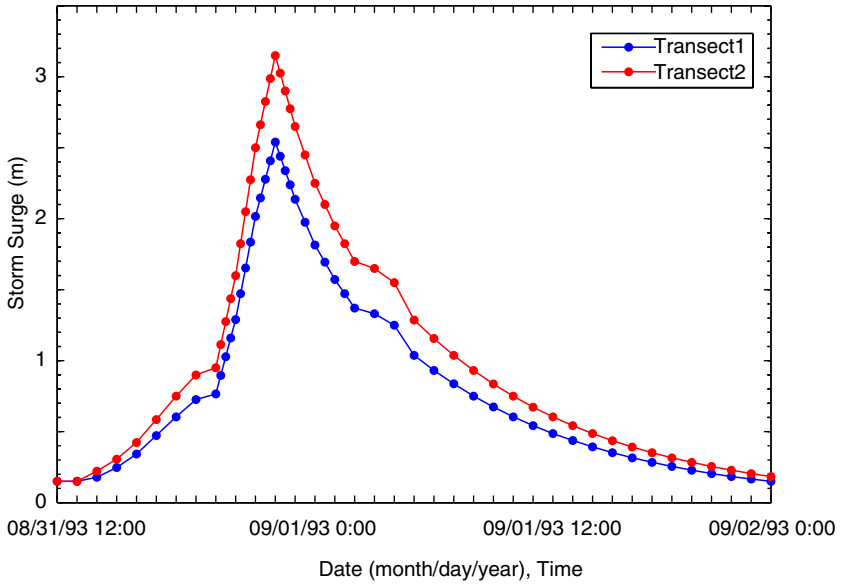

Fig. 4 Pamlico Sound water levels at transects 1 (Frisco) and 2 (Buxton) during Hurricane Emily, August 31 and September 1, 1993. Modified from Peng et al. (2004)

sound levels, which are used as the lateral boundary conditions in all nodes representing Pamlico Sound during the calibration simulations at both transects. This sound surge acts as a pulse source of saline water to the aquifer, flooding much of the low-lying land adjacent to Pamlico Sound, including the Frisco Wellfield. Flood waves are simulated in a piece-wise linear fashion on the sound side of the model domain. Nodes along the top boundary that lie below the elevation of the flood wave receive a source of saline water through the assignment of (1) constant pressure boundary conditions related to the height of standing water; and (2) constant concentration boundary conditions at the concentration of Pamlico Sound rather than assuming a fluid source at a certain concentration. Time steps during storm events were 300 s and the typical length of simulation at any particular flooding level varied from 900 to 3,600 s. The simulation of the rise and fall of the Hurricane Emily flood wave, for example, involved 60 separate simulations. The simulation of shorter flooding events during the historical simulations involved fewer separate simulations.

Model calibration at transect 1

Calibration simulations at transect 1 attempted to match the TDS breakthrough data by averaging the nodes corresponding to the pumping well's screen and gravel pack. Pumping rates in the months following the hurricane are known (J. Coleman, Cape Hatteras Water, personal communication, 1996) and recharge rates were varied in order to match known water levels. Ultimately, the best fit to the TDS breakthrough data obtained by minimizing the root mean square error (RMSE) occurred with longitudinal dispersivities in the maximum and minimum permeability directions of 10 and 5 m, respectively, and transverse dispersivities in the maximum and minimum permeability directions of 1 and 1 m, respectively. These values are similar in magnitude to those used by Underwood et al. (1992), Ataie-Ashtiani et al. (1999), and Smith (2004) in simulations using SUTRA. Figure 5a shows the calibrated breakthrough curve during the 4 months following the hurricane. In addition to showing the seven observation nodes corresponding to the screened interval, the blue line represents the average concentration of the mixed water entering the water treatment plant as raw water. Measured water-table elevations before and immediately after the hurricane were also used in model calibration, primarily as a means of determining recharge rates. Figure 5b shows the simulated water-table hydrograph and field water-table observations at transect 1 during and immediately after the hurricane. Simulations are able to match the water-table elevations in MW 1-1 during the first 30 d and at 120 d after the storm. Although data are lacking between 30 and 120 d, care was taken to include a large storm at 38 d.

Model calibration at transect 2

Due to a lack of breakthrough data at transect 2, calibration simulations at this location utilized the calibrated dispersivities from transect 1 and calibrated recharge rates to minimize differences between simulated and measured water-table elevations immediately before and after the hurricane. Figure 6 shows calibrated simulations at transect 2. While this figure lacks the TDS breakthrough data shown in Fig. 5, it should be noted that there is excellent agreement between simulated and observed water-table elevations along transect 2.

Model sensitivity simulations

Model sensitivity simulations were performed along transect 2 in order to avoid the pumping effects that exist along transect 1. Each sensitivity simulation received the same

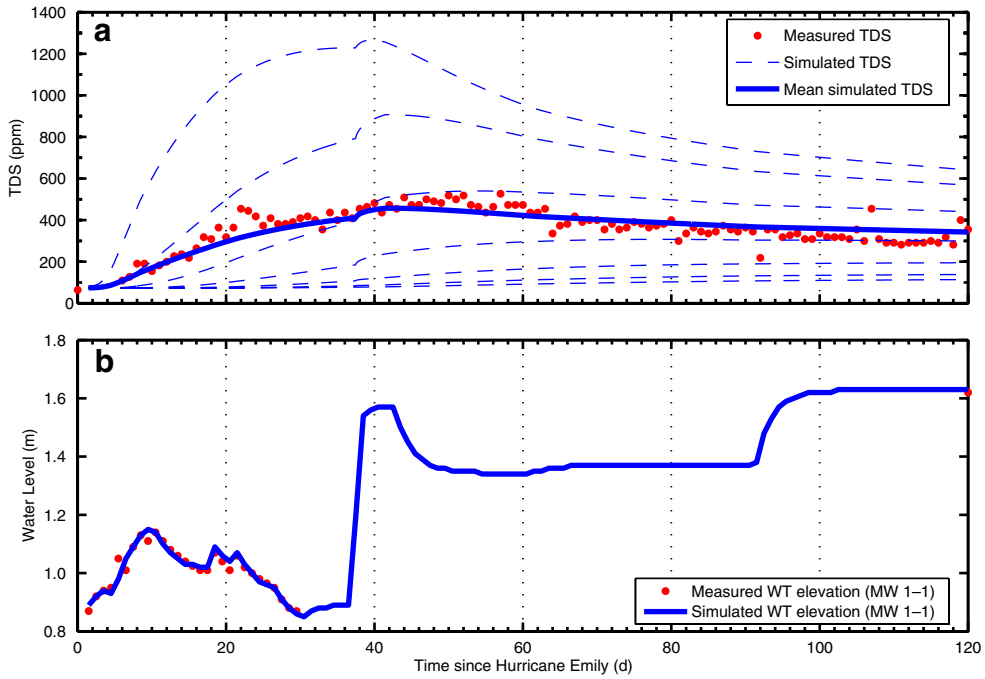

Fig. 5 **a** TDS breakthrough and **b** water-table elevation calibrations for simulations along transect 1

flood-wave signal as was used in the calibration simulations with the exception of the flood-wave sensitivity simulations. Breakthrough curves observed at shallow depth in monitoring well MW 2-1 show model sensitivity to variations in permeability, dispersivity, porosity, flooding duration, and leakage through the base of the aquifer. Figure 7 shows the results of the model sensitivity analysis. Each panel in the figure shows the calibrated simulation as a means of comparison. The model output suggests that (1) the most sensitive parameters are permeability and dispersivity (Fig. 7a and b); and (2) moderately sensitive parameters are porosity, leakage, and flood-wave duration (Fig. 7c–e).

Figure 7a shows model sensitivity to variations in permeability, which were increased and decreased from calibrated parameters by an order of magnitude. Model output demonstrates that this is a highly sensitive parameter, especially when considering higher permeabilities, which enable the pulse of saline water to penetrate deep into the aquifer in a relatively short amount of time. Given the amount of aquifer testing that has been performed on the Buxton Woods aquifer (see Burkett 1996), the high sensitivity of this parameter and the use of aquifer test values lends confidence to the values that are used in subsequent historical simulations. The other highly sensitive parameter is dispersivity, which is shown in Fig. 7b. Increasing this parameter by an order of magnitude allows the TDS pulse to spread out relatively rapidly, leading to higher salinities at depth at earlier times. Decreasing the dispersivity by an order of magnitude has a modest impact on model output. As with permeability, the highly sensitive nature of this parameter lends credibility to the calibration.

Changes in porosity, leakage through the aquifer base, and flood-wave duration all have less influence on model output. Figure 7c shows model sensitivity to changes in porosity. The most significant changes caused by varying this parameter occur in the days immediately following Hurricane Emily; however, these changes are smaller in magnitude than those simulated for permeability and dispersivity and decrease with time. Figure 7d shows the

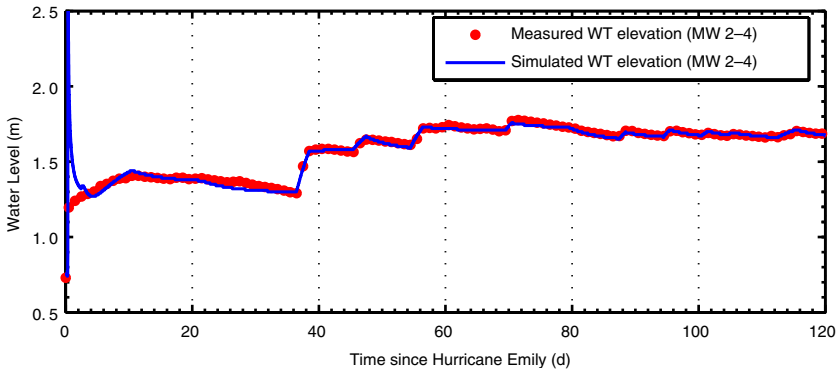

Fig. 6 Water-table elevation calibration for simulations along transect 2

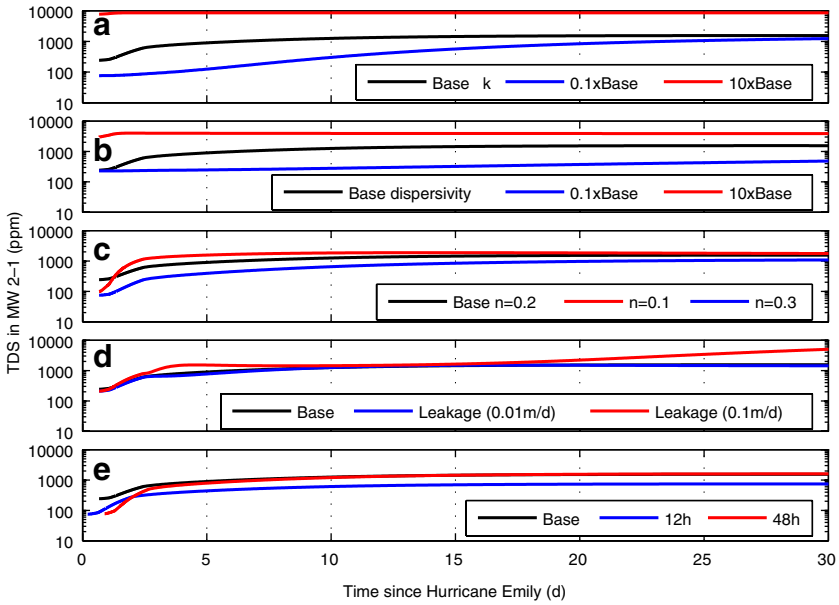

Fig. 7 Sensitivity simulations along transect 2 including sensitivity with respect to **a** permeability (k), **b** dispersivity, **c** porosity, **d** aquifer leakage through the base, and **e** duration of the storm event

sensitivity of model output to changes in the basal boundary condition of the model domain. While the calibration simulations utilize a no-flow boundary at the base of the aquifer, Burkett (1996) found a small amount of leakage through the base of the aquifer during aquifer testing. To test the effect of leakage through the base on the configuration of the mixing zone, sensitivity simulations allowed leakage through the base of the aquifer at rates of 0.01 and 0.1 m/d. As is demonstrated in the figure, this has minimal affect on the simulated breakthrough curves at low leakage rates, but shows more significant variations at late times for high leakage rates. Figure 7e shows model sensitivity to changes in the duration of the flood wave. The simulations of Peng et al. (2004) assume a hurricane translation velocity of 25 km/h. Given that hurricanes and other tropical and extra-tropical storms will likely move at a variety of translation speeds, this series of simulations applies the flood-wave signal over time periods of 12 and 48 h, which represent faster and slower translation times, respectively, than the actual hurricane's duration of 36 h. The sensitivity simulations suggest that translation speed affects model output, most notably for the faster translational speed, which limits the amount of salt recharging the aquifer.

Transient predictive simulations

The calibrated model described above is able to match groundwater flow and solute transport conditions in the Buxton Woods aquifer during and following Hurricane Emily. In order to demonstrate the role that storm events play in defining the morphology of the mixing zone, this section describes two situations: (1) temporal and spatial variations in TDS concentrations in the years following Hurricane Emily, assuming that no other storms have occurred; and (2) temporal and spatial variations in TDS concentrations over a 54-year history of hurricanes, tropical storms, and extra-tropical storms in the Cape Hatteras region. All simulations described in this section are performed along transect 2.

Hurricane Emily's effect on the mixing zone at transect 2

Hurricane Emily was an extreme storm event for the Cape Hatteras region resulting in over 3 m of storm surge in the Buxton area. In addition to being a category 3 storm, Hurricane Emily traveled on a storm track that maximized sound-side flooding effects (Peng et al. 2004). Anderson (2002) calibrated a simple one-dimensional analytical transport model to demonstrate the effects of hurricanes of this magnitude on maximum chloride concentrations in a barrier-island aquifer; however, these simple analytical simulations do not show temporal and spatial variations in the morphology of the mixing zone that were caused by this storm, nor do they demonstrate the typical behavior of the aquifer to more benign storm events. In the current study, simulations of mixing zone morphology were done for the 10 years following Hurricane Emily with the assumptions that (1) no other overwash events affected the aquifer during this time, and (2) no other storm events had occurred previously. This transient simulation uses the aquifer parameters shown in Table 1 as well as the calibrated dispersivity values. Because water-level data at this location do not exist for much of the 10 years of simulation time, the model uses a recharge rate that produces water-table elevations that match mean water levels at observation well MW 2-4, which was used in the transect 2 calibration simulations. This recharge rate is based on an average water-table elevation calculated from 3 years of high-frequency monitoring data (Anderson and Evans 2007). In addition, because the effects of previous

storms on the mixing zone are unknown, these simulations assume a background TDS concentration of 73 mg/L throughout the aquifer.

Figure 8 shows simulated breakthrough curves at the four observation locations in the model domain. Monitoring wells 1–4 (MW 2-1, MW 2-2, MW 2-3, MW 2-4) occur at simulated distances from Pamlico Sound of 200, 520, 860, and 1,000 m, respectively. In addition to measuring TDS breakthrough at the water table, observation points also monitor simulated breakthrough at depths of 5, 10, and 15 m below MSL in order to demonstrate spatial and temporal TDS variations.

MW 2-1 (Fig. 8a) lies on a low dune 200 m from Pamlico Sound. Initial condition simulations suggest that the typical pre-storm hypothetical TDS concentration at this site is 73 mg/L. The dune creates a thick unsaturated zone relative to other observation locations in the simulation, which insulates the shallow monitoring point from approaching sound-level TDS concentrations during the overwash event; however, once the TDS pulse reaches the water table, concentrations peak and begin a long decay process. After 10 years of simulation time, TDS concentrations are near 500 mg/L, which is approximately seven times the hypothetical pre-storm level.

MW 2-2 (Fig. 8b) lies in an interdunal swale that intersects Pamlico Sound and serves as a conduit for storm surge. This location, coupled with a thin unsaturated zone, creates a high peak TDS concentration of approximately 5,000 mg/L. This is the highest peak value of the four shallow (water table) monitoring locations. MW 2-2–MW 2-4 also have hypothetical initial TDS concentrations of 73 mg/L. After 10 years of simulation time, TDS concentrations at MW 2-2 are approximately eight times their hypothetical value. MW 2-3 (Fig. 8c) and MW 2-4 (Fig. 8d), both further inland, show decreasing levels of TDS breakthrough. At MW 2-3, peak concentrations at the water-table monitoring point are near 2,500 mg/L. After 10 years of simulation time, TDS concentrations are still three times that of the initial conditions. At MW 2-4, peak concentrations at the water-table monitoring point exceed 1,200 mg/L and are still 1.3 times initial values 10 years after the hurricane event.

Figure 9 shows the simulated mixing zone morphology under initial conditions and at various times (pre-storm, 1 d, 1 week, 1 month, 1 year, and 10 years) after the flooding event. All of the plots in this figure show TDS as a fraction of Pamlico Sound TDS. The TDS pulse from this single storm event is persistent, especially when comparing results to pre-storm levels (Fig. 9a). At the end of the flooding event, approximately 1 day after the beginning of the storm surge, TDS values in the near surface are greater than 50% that of Pamlico Sound (Fig. 9b). These simulated values are corroborated by field samples collected during a field trip to Hatteras Island 3 d after the hurricane (Mew HE, North Carolina Department of Environment, Health, and Natural Resources, 1993). This slug of saline water infiltrates the aquifer and diminishes in concentration as it disperses. Within approximately 1 year of the hurricane event (Fig. 9e), the saline plume has infiltrated through the entire thickness of the aquifer at MW 2-1 and MW 2-2. At MW 2-3 and MW 2-4, however, full mixing does not occur until 2 years after the pulse TDS source has been applied. Even after 10 years of simulation time (Fig. 9f), the aquifer has still not returned to pre-storm TDS levels. In fact, the 1% sound water TDS contour is still approximately 500 m inland of its hypothetical pre-storm position.

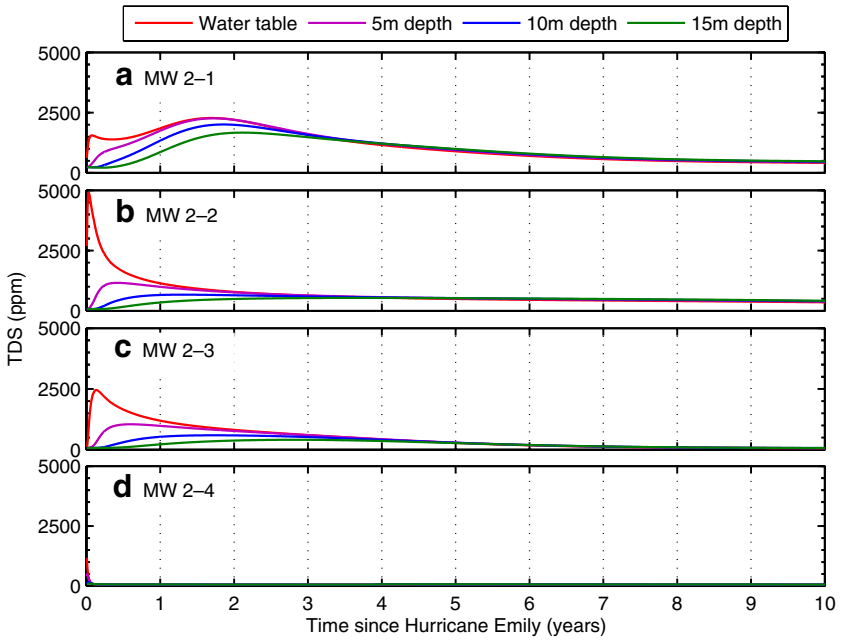

Fig. 8 TDS breakthrough curves after Hurricane Emily as simulated at four observation locations along transect 2 including **a** MW 2-1 (200 m), **b** MW 2-2 (520 m), **c** MW 2-3 (860 m), and **d** MW 2-4 (1,000 m)

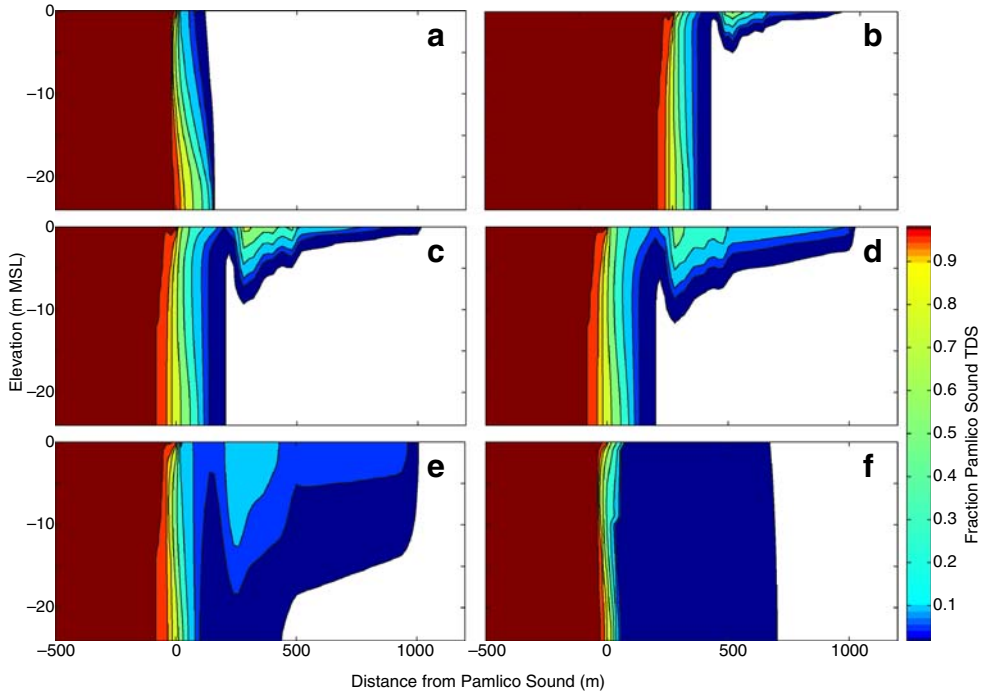

Fig. 9 Mixing zone morphology as simulated at five different times after Hurricane Emily along transect 2: **a** initial conditions, **b** 1 d, **c** 1 week, **d** 1 month, **e** 1 year, and **f** 10 years. Contours are displayed as a percentage of the TDS of Pamlico Sound, which is typically 19,000 ppm or approximately 53% that of seawater

The preceding discussion has only considered conditions in the Buxton Woods aquifer after a single and significant hurricane event; however, it is well known that hurricanes and other storm events occur quite frequently in the Cape Hatteras region. Therefore, while the previous simulations successfully demonstrate the effect of a large storm event, they are limited in the sense that they do not consider the influence of multiple storm events on the mixing zone configuration at transect 2. It is suggested that a continuum of storm events would more accurately represent the behavior of this system, and would lead to a more realistic simulation of the mixing zone configuration. The discussion in the following section attempts to define a more "average" mixing zone configuration in light of this continuum.

The effect of 54 years of storm activity on the mixing zone at transect 2

Peng et al. (2004) modeled storm effects in Pamlico Sound based on historical tracks of hurricanes and other large storms affecting the Cape Hatteras region. They note that the Cape Hatteras region experiences these storms in orientations primarily approaching from the south and southwest and run their simulations using five different locations in each approaching direction. Because the goal of Peng et al. (2004) is to predict coastal flooding throughout Pamlico and Albemarle Sounds with the various storm tracks and for large storms, the authors simulate category 2 and 3 hurricanes that approach the coast at a translation velocity of 25 km/h. Their model output consists of maps of Pamlico and Albemarle Sounds with predicted sound-level contours shown at 2-hour increments.

The current study uses the model output of Peng et al. (2004) to create sound-side boundary conditions in simulations of 54 years of sound-side flooding history at transect 2. NOAA annual hurricane summaries from 1951 to 2006 were used to identify storms that affected the Cape Hatteras region. These storm events were assigned to a particular storm-track orientation of Peng et al. (2004), whose model outputs were used to create sound-level time series for use as lateral and upper boundary conditions in the simulated Pamlico Sound.

Because Peng et al. (2004) modeled only category 2 and 3 hurricanes, and those are relatively rare over the 54 years of record, this study reduced the magnitude of storm surge by a factor equivalent to the ratio of predicted category 2 levels to predicted category 3 levels. For example, storms approaching from the south along a track coincident with the 75°W longitude (Peng's track No. 4, which is the path of Hurricane Emily) have a predicted maximum storm surge in the Cape Hatteras region of ~2 m under category 2 conditions but ~3 m under category 3 conditions (Peng et al. 2004). Thus, this study uses the ratio of 0.67 along this track to reduce overwash amounts for decreasing storm intensities, giving a value of 1.33 m for a category 1 hurricane, 0.88 m for a tropical storm, etc. Table 2 shows storm tracks, category 2 to category 3 ratios, and overwash levels for the eight storm

Table 2 A summary of the storm tracks that affected the Cape Hatteras, NC, region between 1953 and 2006. Surge levels indicate the maximum level of storm surge for a particular storm track (Peng et al. 2004)

	Storm track 2	Storm track 3	Storm track 4	Storm track 5	Storm track 6	Storm track 7	Storm track 8	Storm track 9
Number of storms	1	6	3	4	5	4	9	11
H2/H3 ratio	0.50	0.84	0.67	0.46	0.72	0.50	0.74	0.88
H3 surge (m)	–	–	2.00	1.00	–	–	–	1.00
H2 surge (m)	0.50	0.84	1.33	0.46	0.94	1.00	2.23	0.88
H1 surge (m)	–	0.71	–	0.21	–	0.50	–	0.77
Tropical storm surge (m)	–	0.59	0.59	–	0.49	0.25	1.23	0.67
Tropical depression surge (m)	–	0.50	–	–	–	–	0.91	0.59
Extratropical storm surge (m)	–	0.50	–	–	–	–	0.91	0.59

tracks affecting transect 2. Data in this table are only shown for those storms that have affected the Cape Hatteras region in the past 54 years. The table also indicates the number of storms that occurred along a given orientation for a total of 43 storms.

Figure 10 shows TDS breakthrough over 54 years of simulation time at the four observation points at all depths, as was shown in Fig. 8 for the Hurricane Emily simulations. The simulation output suggests that TDS levels in the Buxton Woods aquifer are highly variable. Note that even the relatively quiescent period of the late 1960s and early 1970s does not provide enough time for TDS levels to return to hypothetical non-storm levels in MW 2-1. The model output also suggests that mean TDS levels in the Buxton Woods aquifer at monitoring points MW 2-1 through MW 2-4 are far from their theoretical pre-storm conditions. Mean TDS values at MW 2-1 through MW 2-4 are approximately 800, 280, 140, and 90 mg/L, respectively. With modeled TDS means under pre-storm conditions at 70 mg/L in MW 2-1 through MW 2-4, theoretical mixing zone values are off by more than a factor of ten within 200 m of Pamlico Sound and by a factor of nearly 1.3 at a distance of 1,000 m from Pamlico Sound.

Modeling discussion

There are several drawbacks to this method of deriving the Pamlico Sound boundary condition. First, all simulated storms are assumed to translate through the region at a rate of 25 km/h as simulated by Peng et al. (2004). Because not all storms move at this translation speed, most of the storms will not produce this sound-level time series. For example, as was shown in the sensitivity simulations, a storm moving at a slower translation speed will likely generate higher surge levels than were simulated by Peng et al. (2004); conversely, a faster translation speed will likely generate lower surge levels than are shown in Table 2. Second, the precision of the storm levels is limited. Peng et al. (2004) provide maps of Pamlico Sound showing water levels at 2-hour increments; thus, the level of detail with which to generate the sound-level

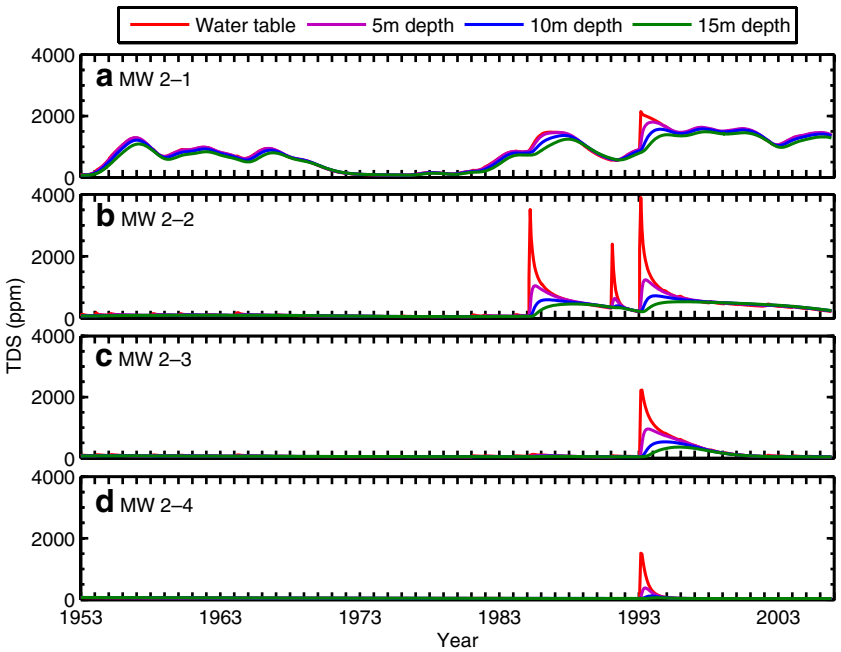

Fig. 10 TDS breakthrough curves over a 54-year period as simulated at four observation locations along transect 2 including **a** MW 2-1, **b** MW 2-2, **c** MW 2-3, and **d** MW 2-4. The beginning date of the simulations is August 13, 1953

time series is limited. Third, not all storms follow a path that corresponds exactly to the storm tracks of Peng et al. (2004). Care was taken to assign each storm to a proper track; however, three of the 43 storms did not match the ten typical storm tracks and were assigned the time series of the closest storm track.

Discussion

Overall, given the approximations of the Pamlico Sound boundary conditions, the simulations described above can be taken as a conservative estimate of mixing zone morphology, and this morphology is quite different than mixing zone theory predicts. In fact, overwash is the principal controlling factor of the simulated mixing zone's morphology. While local heterogeneities and seasonal and interannual recharge variations may cause minor variations in the morphology of the mixing zone, the magnitude of their effects would be smaller in scale. Figure 11a shows a plot of average mixing zone conditions based on the average model output of the 54-year simulation at the simulated monitoring wells. The figure indicates that the mixing zone is considerably wider than that predicted by theory. For example, compare the average mixing zone to the steady-state non-storm configuration shown in Fig. 11b. The 1% sound water TDS contour in the average mixing zone configuration is approximately 500 m inland of the hypothetical non-storm configuration.

Many studies in the literature suggest that tidal oscillations and other parameters such as wave run-up are important factors in determining the shape of the mixing zone (see, for example, Ataie-Ashtiani et al. 1999). Tidal oscillations, when coupled with aquifer parameters such as permeability, are the primary driving force in establishing the configuration of the mixing zone. It should be noted that many of these studies (see, for example, Underwood et al. 1992) were done on atolls where the underlying limestone aquifer is highly permeable. On Hatteras Island and many other barrier islands, however, permeabilities are an order of magnitude or more lower than those of most atolls and the tidal signal is unable to penetrate very far inland. In addition, the

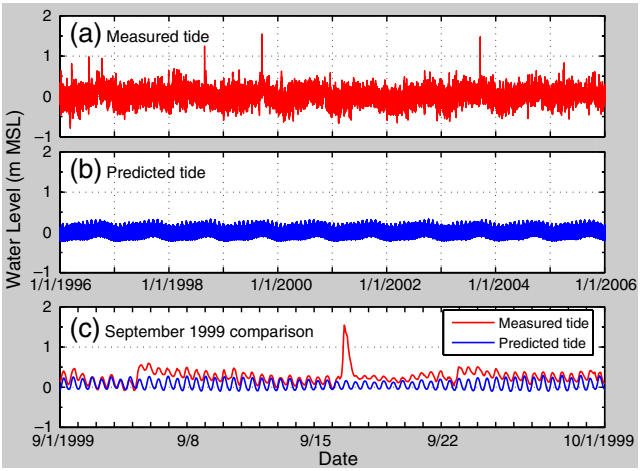

Fig. 12 A comparison between **a** measured and **b** predicted tidal oscillations at Oregon Inlet as measured at the NOAA Oregon Inlet Tide Gauge near Oregon Inlet, North Carolina. The bottom panel **c** zooms in on predicted and measured water levels during September 1999, which is an active month for tropical storms

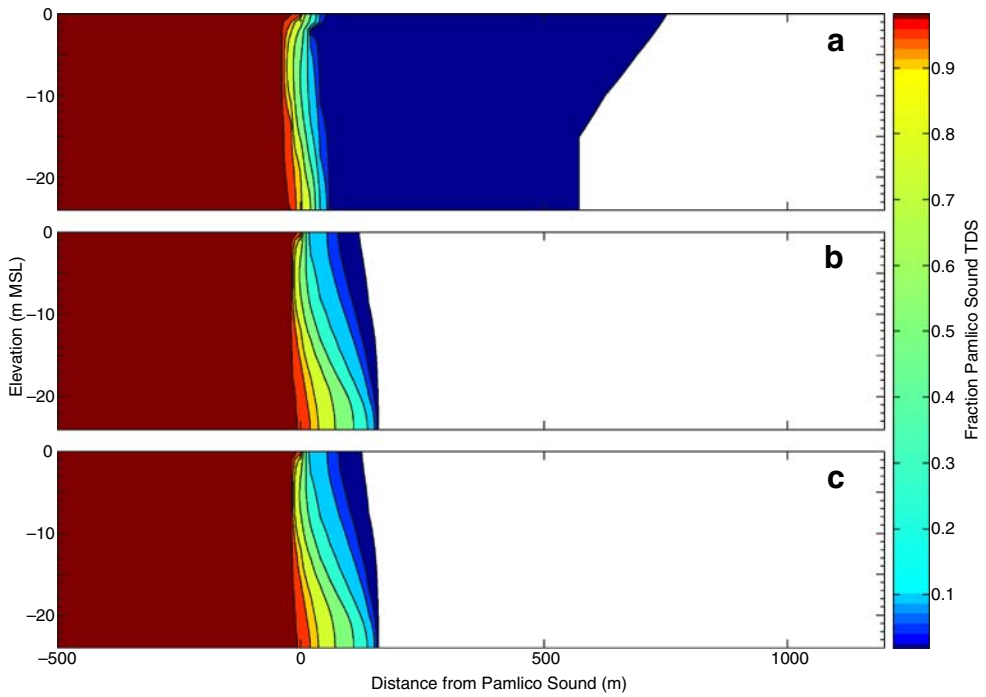

Fig. 11 Simulated mixing zone morphologies based on **a** average simulated conditions over 54 years, **b** pre-storm conditions, and **c** pre-storm conditions with a tidal boundary condition in Pamlico Sound. *Contours* are displayed as a percentage of the TDS of Pamlico Sound, which is typically 19,000 ppm or approximately 53% that of seawater

microtidal nature of some barrier islands makes the tidal signal even less important. Hatteras Island is one such microtidal barrier island with a tidal amplitude of only 15 cm on the sound side of the island. Figure 11c shows the mixing zone configuration along the island's boundary with Pamlico Sound under tidal conditions. Note that there is no difference between the mixing zone configurations of Fig. 11b and c. Tidal oscillations were also not simulated on the ocean side of the island, where their influence would likewise be minimal.

While tidal oscillations play a minimal role in mixing zone formulation in microtidal barrier islands (Anderson 1999), especially along the lagoon sides of these islands, this study demonstrates that basic wind events play a more important role. Simulations by Peng et al. (2004) illustrate that sound-level variations produced by storm events such as hurricanes, tropical storms, and extratropical storms are dramatically larger than predicted tidal oscillations. Data collected by the National Oceanic and Atmospheric Administration at a tidal gauge in Pamlico Sound at Oregon Inlet (Fig. 12), which is the closest tidal gauge to the study site, show that wind events, even small events that occur on a daily basis, have much more of an effect on sound levels than do predicted tidal oscillations—data downloaded from NOAA (2007) with a search for Oregon Inlet Tide Gauge. Simulations in this study demonstrate the role that these wind events play in providing a source of saline water as instantaneous saltwater intrusion from above; thus, from a water-management perspective, care should be taken in making assumptions about the quantity of freshwater in a coastal aquifer based on mixing zone theory. While predicted tidal oscillations at Buxton and Frisco would be similar to the predicted NOAA dataset from Oregon Inlet, the wind-induced oscillations at Buxton and Frisco would likely be considerably more extreme than those at Oregon Inlet due to higher fetch at the southern end of Hatteras Island.

Most people live on the lagoonal sides of barrier islands, and this is especially true of the study site presented in this paper. Coastal flooding of these low-lying, lagoonal regions during storm events causes a mixing of not only saline waters from the lagoon or sound with the freshwater aquifer, as has been demonstrated in this paper, but also a mixing of the circulating and recharged flood waters with all of the products of a modern civilization such as septic systems, and oil, grease, and other contaminants from roadways. The high gradients produced in the groundwater flow system through the instantaneous recharge of these flood events raises the velocity of submarine groundwater discharge in the near-shore environment and may have considerable impact on near-shore water quality. Simulated peak groundwater velocities along the Pamlico Sound shoreline vary from a low of 3.5×10^{-06} m/s during hypothetical pre-storm conditions to a peak value after the flood wave of 8.0×10^{-06} m/s. These values subside somewhat after the flood wave recedes, but the rapid rate of recharge caused by the storm produces a simulated groundwater velocity of approximately two times the pre-storm rate for several months after the storm event. While submarine groundwater discharge and a detailed analysis of the velocity field is beyond the scope of this paper (see Smith 2004 and Prieto and Destouni 2005 for examples of submarine groundwater discharge research), the effect that storm events have on discharge rates is a problem that needs to be addressed in future studies.

Acknowledgements The authors would like to thank the Thomas F. and Kate M. Jeffress Memorial Trust for funding a portion of this study. They would also like to thank J. Coleman, formerly of the Cape Hatteras Water Association, for providing water quality and pumping data. In addition, the authors would like to thank G. O. Essink, L. Lebbe, D. Evans, and an anonymous reviewer for insightful comments which greatly improved this manuscript.

References

Anderson WP Jr (1999) The hydrology of Hatteras Island. PhD Thesis, North Carolina State University, USA

Anderson WP Jr, Evans DG, Snyder SW (2000) The effects of Holocene barrier-island evolution on water-table elevations, Hatteras Island, North Carolina, USA. Hydrogeol J 8:390–404

Anderson WP Jr (2002) Aquifer salinization from storm overwash. J Coast Res 18:413–420

Anderson WP Jr, Evans DG (2007) On the interpretation of recharge estimates from steady-state model calibrations. Ground Water 45:499–505. doi:10.111/j.1745–6584.2007.00312.x

Ataie-Ashtiani B, Volker RE, Lockington DA (1999) Tidal effects on sea water intrusion in unconfined aquifers. J Hydrol 216:17–31

Bear J (1972) Dynamics of fluids in porous media. Dover, New York

Burkett CA (1996) Estimating the hydrogeologic characteristics of the Buxton Woods Aquifer, Hatteras Island, North Carolina. MSc Thesis, North Carolina State University, USA

Collins WH III, Easley DH (1999) Fresh-water lens formation in an unconfined barrier-island aquifer. J Am Water Res Assoc 35:1–21

Domenico PA, Schwartz FW (1990) Physical and chemical hydrogeology. Wiley, New York

Drabbe J, Badon Ghyben W (1888–1889) Nota in verband met de voorgenomen putboring nabij Amsterdam [Memorandum in connection with the intended well drilling near Amsterdam]. Tijdschrift van het Koninklijk Instituut van Ingenieurs [Periodical of the Royal Institute of Engineers], The Hague, pp 8–22

Freeze RA, Cherry JA (1979) Groundwater. Prentice-Hall, Englewood Cliffs, NJ

Giese GL, Wilder HB, Parker GG Jr (1979) Hydrology of major estuaries and sounds of North Carolina. US Geol Surv Water Resour Invest Rep 79–46:1–175

Heath RC (1988) Groundwater resources of the Cape Hatteras Area of North Carolina: a report to the Cape Hatteras Water Association, Inc. Cape Hatteras Water Association, Buxton, NC

Heath RC (1990) Report on the proposed Buxton Woods wellfield of the Cape Hatteras Water Association. Cape Hatteras Water Association, Buxton, NC

Herzberg A (1901) Die Wasserversorgung einiger Nordseebader [The water supply of parts of the North Sea coast in Germany]. J Gasbeleuchtung Wasserversorgung 44:815–819 and 45:842–844

Krantz DE, Manheim FT, Bratton JF, Phelan DJ (2004) Hydrogeologic setting and ground water flow beneath a section of Indian River Bay, Delaware. Ground Water 42:1035–1051

Li L, Barry DA, Stagnitti F, Parlange J-Y (2000) Groundwater waves in a coastal aquifer: a new governing equation including vertical effects and capillarity. Water Resour Res 36:411–420

Luettich RA Jr, Carr SD, Reynolds-Fleming JV, Fulcher CW, McNinch JE (2002) Semi-diurnal seiching in a shallow, microtidal lagoonal estuary. Cont Shelf Res 22:1669–1681

Manheim FT, Krantz DE, Bratton JF (2004) Studying ground water under Delmarva coastal bays using electrical resistivity. Ground Water 42:1052–1068

NOAA (2007) http://tidesandcurrents.noaa.gov. Cited September 2007
Peng M, Xie L, Pietrafesa LJ (2004) A numerical study of storm surge and inundation in the Croatan-Albemarle-Pamlico Estuary System. Estuar Coast Shelf Sci 59:121–137
Pietrafesa LJ, Janowitz GS, Chao T-Y, Weisberg RH, Askari F, Noble E (1986) The physical oceanography of the Pamlico Sound. UNC Sea Grant Publication UNC-WP-86–5, UNC Sea Grant, Raleigh, NC
Prieto C, Destouni G (2005) Quantifying hydrological and tidal influences on groundwater discharges into coastal waters. Water Resour Res 41, W12427. doi:10.1029/2004WR003920
Roelofs EW, Bumpus DF (1953) The hydrography of Pamlico Sound. Bull Mar Sci Gulf Caribb 3:181–205
Smith AJ (2004) Mixed convection and density-dependent seawater circulation in coastal aquifers. Water Resour Res 40, W08309. doi:10.1029/2003WR002977
Underwood MR, Peterson FL, Voss CI (1992) Groundwater lens dynamics of atoll islands. Water Resour Res 28:2889–2902
Vandenbohede A, Lebbe L (2006) Occurrence of salt water above fresh water in dynamic equilibrium in a coastal groundwater flow system near De Panne, Belgium. Hydrogeol J 14:462–472
Voss CI (1984) SUTRA: a finite-element simulation model for saturated-unsaturated fluid-density-dependent ground-water flow with energy transport or chemically-reactive single-species solute transport. US Geol Surv Water Resour Invest Rep 84–4369
Voss CI, Provost AM (2002) A model for saturated-unsaturated, variable-density ground-water flow with solute or energy transport. US Geol Surv Water Resour Invest Rep 02–4231
Voss CI, Souza WR (1987) Variable density flow and solute transport simulation of regional aquifers containing a narrow freshwater-saltwater transition zone. Water Resour Res 23:1851–1866
Wilder HB, Robison TM, Lindskov KL (1978) Water resources of northeast North Carolina. US Geol Surv Water Resour Invest Rep 77–81:1–113
Wilson AM, Gardner LR (2006) Tidally driven groundwater flow and solute exchange in a marsh: numerical simulations. Water Resour Res 42, W01405. doi:10.1029/2005WR004302